Available online at www.sciencedirect.com

ScienceDirect

Ceramics International 40 (2014) 273–280

CERAMICS INTERNATIONAL

www.elsevier.com/locate/ceramint

Fabrication of zirconia-toughened alumina parts by powder injection molding process: Optimized processing parameters

Sarizal Md Ani, Andanastuti Muchtar*, Norhamidi Muhamad, Jaharah A. Ghani

Department of Mechanical and Materials Engineering, Faculty of Engineering and Built Environment, Universiti Kebangsaan Malaysia, 43600 UKM Bangi, Selangor, Malaysia

Received 21 April 2013; received in revised form 4 May 2013; accepted 22 May 2013
Available online 13 June 2013

Abstract

Zirconia-toughened alumina (ZTA) parts were fabricated by using a powder injection molding process that utilizes a multi-component binder system based on high-density polyethylene, paraffin wax, and stearic acid. The entire aspect of the manufacturing process, which includes mixing, injection molding, debinding, and sintering, were optimized in this study. ZTA powder was mixed with binders at powder loading ranging from 53 vol% to 59 vol%. The optimum powder loading was determined by analyzing the rheological properties and homogeneity of feedstocks. During injection molding, the temperature and injection pressure parameters were manipulated to obtain optimum density results. A two-stage debinding process (solvent and thermal) was used to remove binders in green parts. Debound parts were sintered at temperatures ranging from 1400 °C to 1600 °C for 2 h. The shrinkage, density, and hardness of the sintered parts were measured. Results show that with homogeneous mixing, the feedstocks were transformed into pseudoplastic in less than 30 min. Powder loading of 57 vol% is the most optimal case for injection molding according to the power law index and flow activation energy values. The theoretical relative density reached 90.27% with defect-free parts under optimum injection temperature and pressure. The weights of the parts decreased by 82.26% during solvent debinding at 60 °C, whereas the binders were completely degraded at approximately 550 °C during thermal debinding. Experimental results also indicate that the shrinkage, density, and hardness reached their maximum values at a sintering temperature of 1600 °C. The sintered parts were densified with approximately 98% theoretical density, hardness of 1582.4 HV, and 15% shrinkage value.

Keywords: A. Injection molding; A. Mixing; C. Mechanical properties; Zirconia-toughened alumina

1. Introduction

Powder injection molding (PIM) is a combination of powder technology and injection molding that involves several stages, including mixing, debinding, and sintering [1]. During mixing, ceramic powder is blended with binders to form a homogeneous compound. Binders provide viscosity to the powder, thereby simplifying the process of filling feedstock into molds during injection molding. In addition, binders help maintain the original shape of the ceramic powder during debinding and until the start of the sintering process [2]. Optimum powder loading ratio is also important in the success of PIM. The powder and binder ratio ranges from 45% to 75% by volume [3]. A high powder loading ratio will cause inconsistencies in the injected parts, which can subsequently damage the injection machine. By contrast, a low powder loading ratio can cause separation of binders from powder during injection, thus prolonging debinding and leading to considerable shrinkage during sintering [4,5]. An optimum percentage of powder loading can minimize shrinkage, prevent cracking, and increase the mechanical properties of materials [6]. Therefore, the rheological properties of feedstock were evaluated to obtain the optimum powder loading ratio for injection.

The combination of solvent and thermal debinding technique has been proven successful in reducing binder decomposition time and in preventing defects in green parts [7–9]. The use of a multi-component binder system allows binder

*Corresponding author. Tel: +60 389118379; fax: +60 389118314.
E-mail addresses: sarizal@eng.ukm.my (S. Md Ani), muchtar@eng.ukm.my, tutimuchtar@gmail.com (A. Muchtar), hamidi@eng.ukm.my (N. Muhamad), jaharah@eng.ukm.my (J.A. Ghani).

0272-8842/$ - see front matter © 2013 Elsevier Ltd and Techna Group S.r.l. All rights reserved.
http://dx.doi.org/10.1016/j.ceramint.2013.05.134

removal in stages (solvent and thermal). Binder removal is important in maintaining the shape of parts, thereby preventing the occurrence of cracking, blistering, and bloating, which may affect the quality of products after sintering [7]. Currently, a method based on powder pressing and slip casting is commonly used in producing zirconia-toughened alumina (ZTA) parts, whereas PIM is still not extensively used. Previous studies have focused only on the use of ceramic powder based on alumina or zirconia materials [6,7,9]. Therefore, this study focused on ZTA ceramic powder because the material properties of ZTA are better than its original nature. A complete PIM process was developed to fabricate cylindrical ZTA parts with the multi-component binder system on the basis of high density polyethylene (HDPE), paraffin wax (PW), and stearic acid (SA). The homogeneity and rheological properties of feedstocks were studied, and the processing parameters for molding, debinding, and sintering were optimized.

2. Material and methods

A combination of alumina and zirconia powders with binders consisting of HDPE, PW, and SA was used as feedstock. The alumina and zirconia powders were mixed at a rate of 80% and 20% by weight, respectively. Alumina powder (AL-160SG-1) with an average particle size of 0.40 μm was supplied by Showa Denko, whereas zirconia powder (KZ-3YF) with an average particle size of 0.35 μm was supplied by KCM Corporation. Table 1 shows the characterization of the binders. Differential scanning calorimetry (DSC) analysis and thermogravimetric analysis (TGA) were conducted to determine the melting and decomposition temperatures of the binders. DSC and TGA were performed on a Mettler Toledo DSC 1 STAR^e System and Netzsch STA 449 F3 Jupiter at a heating rate of 10 °C/min.

Prior to mixing, ceramic powder was dried in an electric furnace (Medcenter Venticell III) at 110 °C for 1 h. The alumina and zirconia powders were mixed by using the dry mixing method (Fritsch Pulverisette 6), which was performed at 100 rpm for 8 h by using a ball mill. The ball to powder ratio was 5:1. The average size and density of ZTA powder after mixing was 0.31 μm and 4.46 g/cm^3, respectively. ZTA powder was mixed with binders by using an internal mixer machine (Brabender W 50 EHT) to produce feedstock. Table 2 shows the powder loading ratio and binder composition used in this study. The composition and combination of binders were based on the study of Thomas-Vielma et al. [7]. Powder loading was set based on the critical powder loading (60.5% volume) obtained through the oil absorption method [10]. The feedstocks were labeled AZ53, AZ55, AZ57, and AZ59 according to their percentage of powder loading. German and Bose stated that the optimum powder loading rate is about 2 vol % to 5 vol% lower than the critical powder loading is [11]. The mixing process was conducted at 140 °C with 20 rpm velocity for 30 min. The feedstock was properly granulated with a crusher after mixing (Strong Crusher TSC-5JP).

Homogeneous mixing of feedstock was determined based on torque information recorded in the internal mixer machine [12]. A lower torque value at steady state indicates homogeneous mixing. The homogeneous mixing of feedstocks can also be determined by measuring the standard deviation of density [13]. The density values for each group were obtained from five different feedstock sections by using a Quantachrome Ultrapycnometer 1000 pycnometer. A small standard deviation indicates homogeneous mixing. Feedstock rheological properties were characterized by using a capillary rheometer machine (Shimadzu CFT-500D). A die with 1 mm diameter and 10 mm length was used ($L/D=10$). Tests on rheological properties of feedstock were performed at temperatures ranging from 150 °C to 170 °C with an applied load of 20–90 kgf. Homogeneous feedstocks with good rheological properties were used for injection molding. Energy-dispersive X-ray spectroscopy (EDX) analysis of feedstock for optimal powder loading was evaluated by using a Zeiss Evo MA10 VPSEM.

A standard screw-type injection molding machine (Battenfeld BA 250 CDC) was used to produce the green parts. Mold cavity

Table 1
Characterization of binders.

Binder	Supplier	Density (g/cm^3)	Melting temperature (°C)	Decomposition temperature (°C)
HDPE	Titan Petchem	0.96	131.78	420–550
PW	Emercy Oleochemicals	0.89	59.53	200–400
SA	Emercy Oleochemicals	0.88	69.83	180–380

Table 2
Composition of feedstocks.

Feedstock tag	ZTA powder/binder (vol%)	Binder (wt%)		
		HDPE	PW	SA
AZ53	53/47	50	46	4
AZ55	55/45			
AZ57	57/43			
AZ59	59/41			

was characterized by a round bar (Ø15 mm × 21 mm). The injection temperature and pressure varied from 150 °C to 170 °C and from 80 MPa to 120 MPa, respectively. The holding pressure conditions were similar to the injection pressure parameters. The injection and holding time were 5 and 10 s, respectively, whereas the cooling time and molding temperature were 10 s and 50 °C, respectively. To obtain optimum density results, the temperature and injection pressure parameters were manipulated. The optimized parameters with defect-free green parts were used for the next process. The density of the green parts was measured by using the Archimedes method (Mettler Toledo MS204S).

A two-stage debinding process (solvent and thermal) was used to remove the multi-component binder system in the green parts. Solvent debinding process was performed by immersing the green parts in *n*-heptane (Merck 104379) solution at temperatures ranging from 50 °C to 70 °C (Medcenter Venticell III). The green parts were immersed every 2 h. The sample was then dried before weighing to obtain the percentage weight loss of the binder. To remove the remaining binder, thermal debinding was performed in argon debinding split furnace (Maju Saintifik RS800/200/200). The thermal debinding profile was designed according to the TGA of the binders. The defect and morphological evaluation of green and debound parts were observed by using an Olympus Stereomicroscope SZ6 and Zeiss Evo MA10 VPSEM, and the carbon and hydrogen contents were measured by a CHN analyzer (Finnigan Flash EA 1112). The optimized parameters for each stage with defect-free debound parts were used for sintering.

Debound parts were sintered at five different temperatures (1400, 1450, 1500, 1550, and 1600 °C) for 2 h with 3 °C/min heating rate in a high temperature furnace (Linn VMK-1800). Shrinkage was calculated by using the dimension method, and the density of the sintered parts was measured by using the Archimedes method with distilled water as medium (Mettler Toledo MS204S). The sintered parts were initially polished before measuring their hardness by Vickers micro-hardness tester (Mitutoyo MVK-H11) with a dwell load of 500 gf. The polished sample was thermally etched at 150 °C under sintering temperature, and the microstructure of the sintered parts was observed with Hitachi SU8020 FESEM.

3. Results and discussion

3.1. Feedstock homogeneity

Homogeneous feedstock preparation is important in facilitating injection moldings because homogeneous mixing affects the rheological properties of materials. The homogeneity of ZTA powder and binder mixture was obtained when the torque values reached a steady state. Fig. 1 shows that feedstock torque curves vary at different powder loadings. The increase in torque values occurred concurrently with increased powder loading. An increase in mixing time before obtaining a homogeneous feedstock indicates the presence of different feedstock viscosities. High ceramic powder content will result in large friction between particles and in high torque resistance on rotor blades with increasing homogeneous mixing period [3].

Results show that powder loading lead to homogeneous mixing in less than 30 min. However, at 59 vol% powder

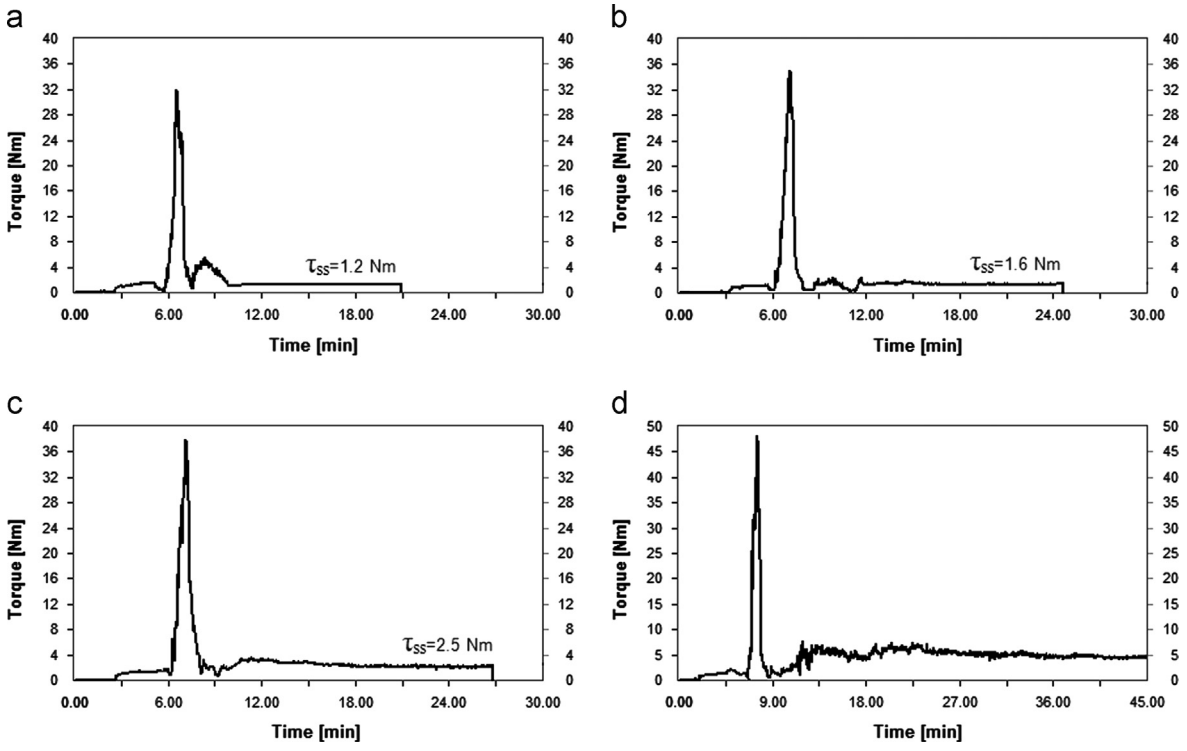

Fig. 1. Torque curve behavior at different volumetric powder loadings: (a) 53, (b) 55, (c) 57, and (d) 59 vol%.

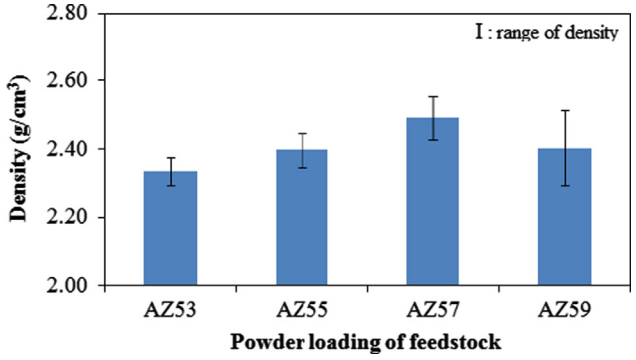

Fig. 2. Density of feedstocks at different powder loadings.

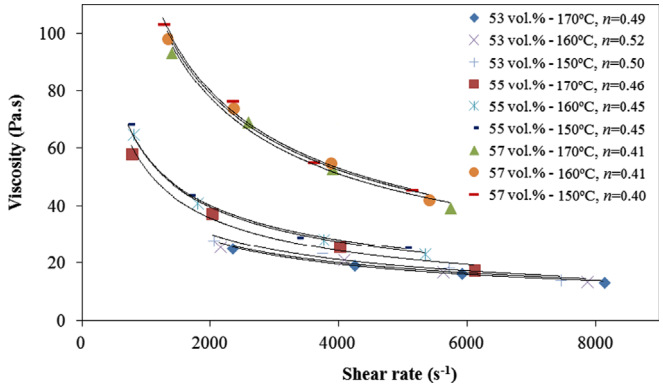

Fig. 3. Effect of powder loading and temperature on viscosity at various shear rates.

loading, the ZTA powder and binder did not mix thoroughly. At higher powder loading, only a certain portion of ZTA powder can be held by the binder even when the mixing time is extended to 45 min. Thus, rheological tests are not applicable to the above case. The homogeneous mixing process was also determined by measuring the standard deviation of the feedstock density, as shown in Fig. 2. Imperfect mixing was observed at 59 vol% powder loading, in which the density was low and the standard deviation was large. A large standard deviation indicates inhomogeneous feedstock mixing, which can result in density gradients within the molded part, causing distortions [13].

3.2. Feedstock rheology

Feedstock rheological characterization was performed to identify the flow characteristics and suitability of feedstock for injection molding. Fig. 3 shows the variation in viscosity of shear rate at different powder loadings and temperatures. All feedstocks exhibited pseudoplastic flow behavior, in which the viscosity values decreased with increasing shear rate. This phenomenon occurred because the lumps that were formed on the feedstock split because of high shear rate, which, in turn, decreases the feedstock viscosity [14]. Pseudoplastic flow behavior shows that binder separation does not occur during injection, thereby minimizing jetting problems. During injection, the feedstock shear rate usually ranges from 10^2 s^{-1} to 10^5 s^{-1} with a maximum viscosity value of up to 10^3 Pa s [13]. The viscosity and shear rates obtained in this study were within the recommended range of 10–100 Pa s and 1000–8000 s^{-1}, respectively.

For pseudoplastic behavior, the power law index (n) is less than 1 ($n < 1$), and the ideal value of n for the feedstock ranges from 0.1 to 0.7 [1]. The value of n was between 0.40 and 0.52 [10]. n refers to the sensitivity of flow to changes in shear rate. A low n indicates a high level of sensitivity, which is suitable for producing small-sized and complex-shaped components [5]. The level of viscosity sensitivity in temperature changes can be correlated to the Arrhenius equation, which is based on flow activation energy (E) [1]. The value of E at 53, 55, and 57 vol% powder loading were 6.24, 4.60, and 1.55 kJ/mol, respectively, indicating that E decreases with increase in powder loading. This phenomenon was driven by better thermal conductivity because of the increase in powder loading in the feedstock [15]. A low E indicates that viscosity is less sensitive to temperature changes and that flow instability during the injection process can be avoided.

The optimum powder loading ratio was determined based on mixing homogeneity and characterization of the rheological properties of feedstocks. At 53, 55, and 57 vol% powder loading, feedstock mixing was found to be homogeneous because of low torque value and steady-state condition with small standard deviation. Given its pseudoplastic nature and low viscosity rate, feedstock is suitable for injection molding. Moreover, 57 vol% powder loading was considered the most optimal for injection molding because of its low power law index and low flow activation energy values. Therefore, problems such as cracking, distortion, and shrinkage of injected parts can be reduced when a powder loading of 57 vol% is used. The feedstock that underwent optimal powder loading contains 19.26 wt% carbon, 31.28 wt% oxygen, 35.97 wt% alumina, and 13.49 wt% zirconia.

3.3. Injection molding

Injection pressure and temperature are important parameters in obtaining a high density, defect-free green part. High density will provide good material properties on the end product, whereas optimum injection pressure will allow feedstock to fill the entire mold cavity [16]. Fig. 4 shows the effects of changes in injection pressure on the density of green parts at different injection temperatures. Experimental results denote that density increases with increasing injection pressure. However, the density stabilized only after the injection pressure reached 110 MPa. These situations occurred in line with a study conducted by Cheng et al., who used a combination of binders similar to the ones used in this study [8]. The binders have higher compressibility than that of ceramic powders at high injection pressure because of the small specific volume of the binder [17]. A high injection pressure resulted in more feedstock being pushed into the mold cavity until the feedstock becomes too dense, causing the density of green parts to become constant.

An increase in injection temperature also influences the density of green parts. Minimal changes in the density of the green part were observed. This result could be caused by the feedstock being less sensitive to temperature changes because of low flow activation energy. In addition, injection pressure and temperature indirectly influenced the quality of the green part. At high injection pressure and temperature, the binders tend to separate and crack on the green part [18]. Furthermore, at high injection temperatures, the feedstock will have low viscosity, which along with high injection pressure will result in easy detachment of binder from the bonds [17]. The residual stresses that exist during shrinkage will lead to the cracking of the green part [19]. Experimental results indicate that the conditions for optimum density of the green part that is free from any defects include an injection temperature of 160 °C with 110 MPa injection pressure and a theoretical density of approximately 90.27%.

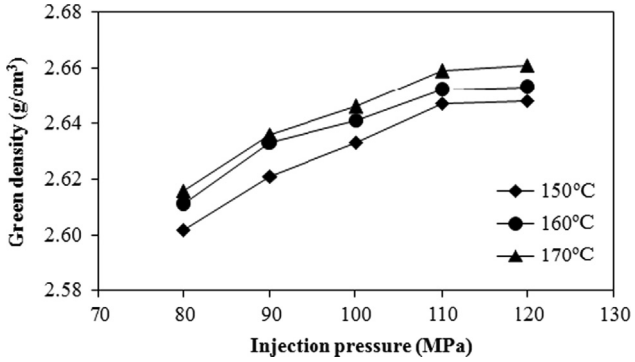

Fig. 4. Effect of injection pressure on the density of the green part at different injection temperatures.

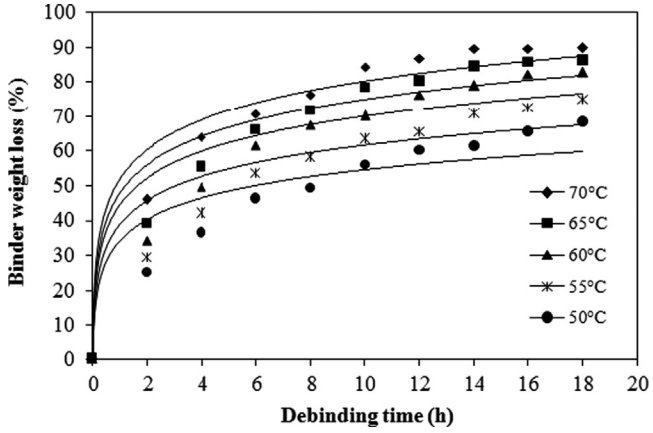

Fig. 5. Effect of solvent debinding temperature on the weight loss of the debound part for various immersion times.

3.4. Debinding process

The binder debinding process for the green part was performed in two stages. At the first stage, the solvent debinding process was performed by soaking the green part into *n*-heptane solution to remove PW and SA. Fig. 5 shows the effect of solvent temperature and immersion time on the weight loss percentage of binder removal. Debinding rate was faster in the early stages and becomes almost steady after 16 h. During the early stages, the binder is in direct contact with the solvent. Then the solvent needs to diffuse deep into the green part before the solvent can dissolve the binder. Cracking occurred at immersion temperatures of 65 and 70 °C. The crack occurred after 2 h of immersion, which can be attributed to the high amount of decomposed binder that is quickly moving out from the body structure at high temperature [20]. Fig. 6 shows the SEM microstructure of debound parts after being immersed at 60 °C with different immersion times.

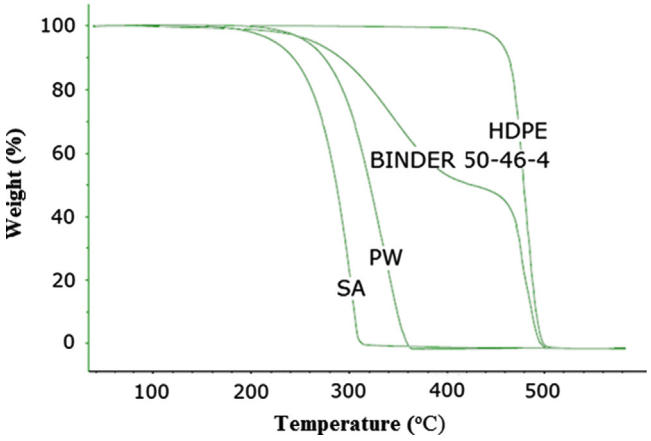

Fig. 7. TGA of the binders.

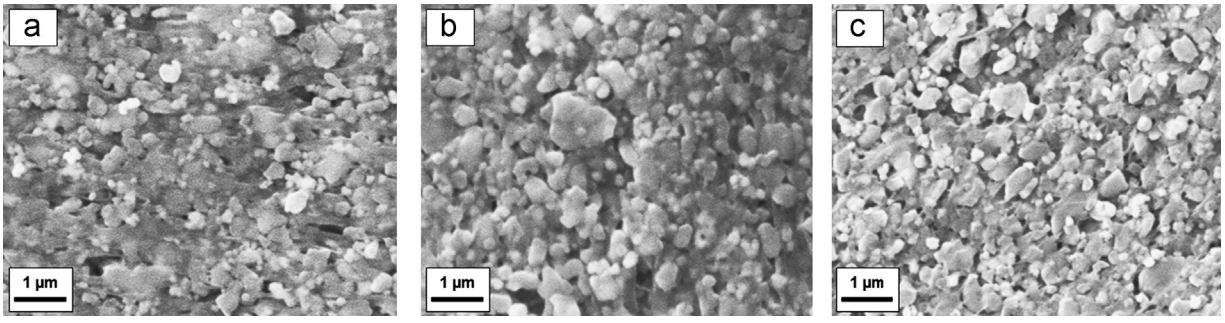

Fig. 6. SEM images of the debound parts after solvent debinding process at 60° C at (a) 0, (b) 2, and (c) 16 h.

Table 3
Optimized thermal debinding schedule.

Stage	Heating rate (°C/min)	Debinding temperature (°C)	Holding time (min)
1	2	420	60
2	1	550	180
3	5	30	0

Table 4
Carbon and hydrogen contents of the debound part.

Content/stage	Before debind	Solvent debinding (60 °C, 2 h)	Solvent debinding (60 °C, 16 h)	Thermal debinding
Carbon (wt%)	12.8	9.0	8.2	0.1
Hydrogen (wt%)	4.2	2.2	1.8	0.1

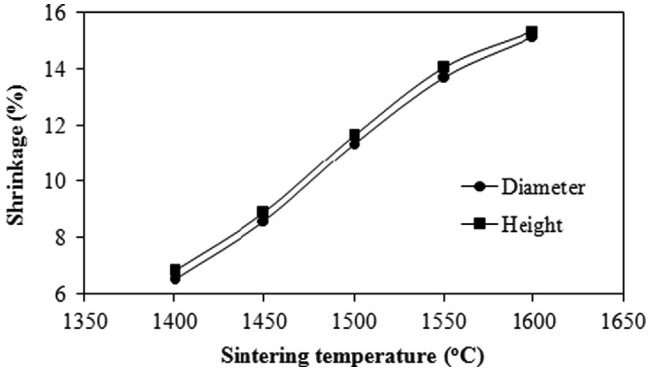

Fig. 8. Effect of sintering temperature on shrinkage.

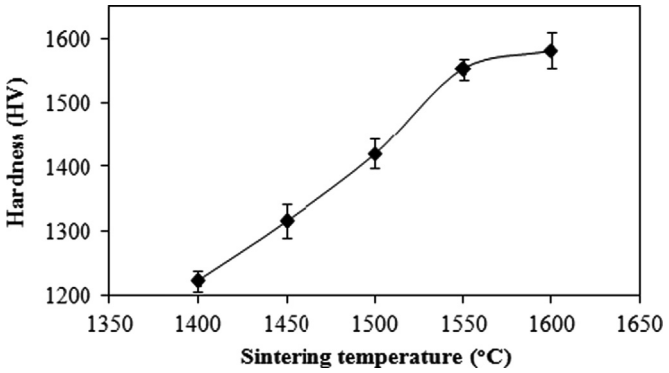

Fig. 10. Effect of sintering temperature on hardness.

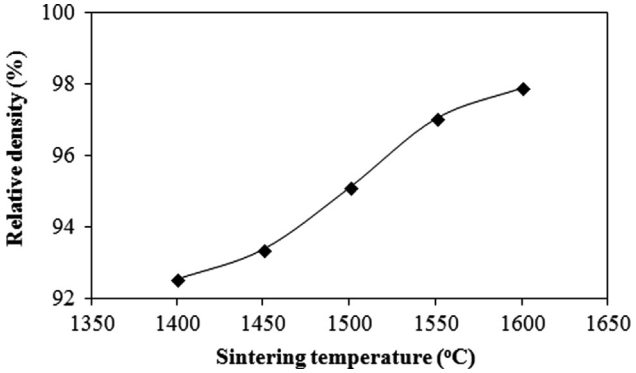

Fig. 9. Effect of sintering temperature on relative density.

The debound parts were free from any defects at these immersion temperatures. The increase in immersion time resulted in the elimination of more PW and SA, thus forming a porous structure. Therefore, an immersion temperature of 60 °C is believed to be the most optimal temperature for solvent debinding. For an immersion period of 16 h, the weight loss of the samples reached 82.26%, resulting in defect-free debound parts.

Thermal debinding process was performed to eliminate HDPE and PW and SA residuals. The debinding schedule for thermal elimination was optimized by TGA of the binders. Fig. 7 shows the TGA of the binders at temperatures ranging from 30 °C to 600 °C. Pure binders decomposed in only one step, whereas multi-component binders require additional steps. All binders were completely degraded at approximately 550 °C. Table 3 shows the optimized thermal debinding schedules. In the first stage of thermal debinding, the residuals of PW and SA were eliminated completely. A slow heating rate was used at temperatures ranging from 420 °C to 550 °C because the HDPE binder began to decompose at this point. Decomposition gases are released through the porous body structure. A high heating rate causes pressure to build up and temperature gradients to occur inside the debound parts, which could result in defects such as cracking, blistering, and bloating [7]. In the second stage, the holding time was extended to 3 h because of the size of the debound parts. SEM results show that almost all of the binders have been decomposed. EDX analysis results show that after debinding, the feedstock consists of 2.77 wt% carbon, 40.29 wt% oxygen, 41.24 wt% alumina, and 15.70 wt% zirconia.

CHN analyzer test was performed to measure the carbon and hydrogen contents of the debound parts. The elemental contents of the binder largely consist of carbon and hydrogen elements. Table 4 shows the carbon and hydrogen content of

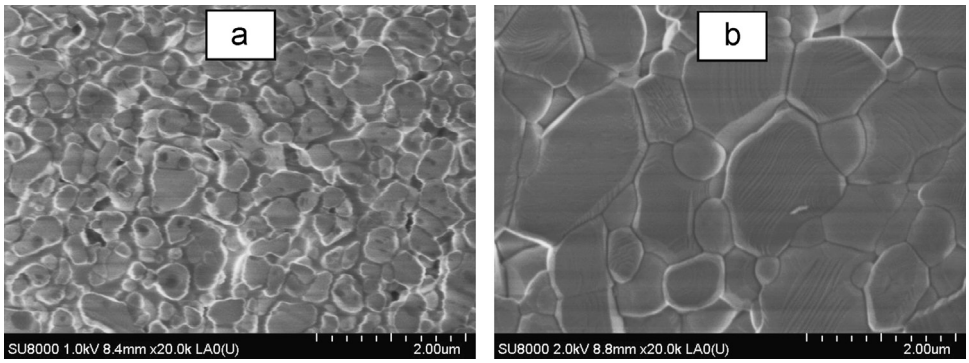

Fig. 11. Microstructure of sintered parts at sintering temperatures of (a) 1400 and (b) 1600 °C

the debound parts, which are 12.8 and 4.2 wt%, respectively before debinding, corresponding to 43 vol% of the binder at 57 vol% powder loading. After solvent debinding from 2 h to 16 h at 60 °C, the carbon and hydrogen content continued to decline. At this point, almost 80% of PW and SA were eliminated. Nearly all binders were decomposed after thermal debinding. The available carbon and hydrogen content in the debound parts were reduced to 0.1 and 0.1 wt%, respectively. The remaining carbon content reported by Foudzi et al. in their study was 0.3 wt% [21]. Thus, the results of the current study indicate that the debinding process was successful. The remaining binder was eliminated completely after sintering.

3.5. Sintering process

Sintering was performed on the debound part to study the effects of temperature changes on shrinkage, density, and hardness. After debinding, no significant change was observed in the sample size. Instead, shrinkage began to occur after sintering (Fig. 8). Experiments show that the percentage of shrinkage increases with increasing sintering temperature on both sides of the sintered part. The results are attributed to the increase in sintering temperature, which causes the pore volume to decrease because of molecular diffusion [22]. The percentage of shrinkage for this experiment ranged approximately from 6% to 15%. On the basis of the powder press method, the shrinkage of the ZTA part was around 17% at a sintering temperature of 1560 °C [23]. The differences in the results were caused by differing composition of ZTA powder and the usage of different binders.

Figs. 9 and 10 show the effects of sintering temperature on the relative density and hardness of the sintered part. The relative density and hardness values for the sintered part increased with increasing sintering temperature. The increase in density values indirectly caused the hardness of the material to become higher. At sintering temperature of 1600 °C, the theoretical relative density reached 97.89%, whereas the hardness values reached 1582.40 HV. The hardness was around 1371 HV when the powder press method was used [23]. The density and hardness values of the sintered parts depend on the strength of the grain boundary. At sintering temperature of 1400 °C, the microstructures still had a cavity space between the particles, as shown in Fig. 11a. The cavity space indicates that the alumina grain has not yet reached complete growth. At sintering temperature of 1600 °C, the alumina grain appeared to have undergone complete growth. Thus, the existing cavity space can be filled with zirconia powder on the interstitial matrix of the alumina, as shown in Fig. 11b. The presence of zirconia powder will prevent irregular alumina grain growth and subsequently reduce the porosity of ceramic materials, which will increase the density and hardness of the material [24].

4. Conclusions

ZTA parts were successfully fabricated through powder injection molding by using binder comprising HDPE, PW, and SA. The results show that almost the entire feedstock achieved homogeneous conditions in less than 30 min with low torque value. The rheological properties of the materials denote that the manufactured feedstock is suitable for injection molding because of its pseudoplastic nature and low viscosity rate. The powder loading of 57 vol% is believed the most suitable for injection molding on the basis of its low power law index and flow activation energy. During injection molding, the optimum density of the green part was achieved at 160 °C injection temperature and 110 MPa injection pressure, which resulted in a defect-free part. All binders in the green parts were successfully eliminated by using a combination of solvent and thermal debinding techniques. The relative density was close to 98% of the theoretical density. A hardness of 1582.4 HV can be achieved by sintering the ZTA parts at 1600 °C. This study shows that PIM is suitable for the production of ZTA parts with good material properties at optimized processing parameters.

Acknowledgments

The authors acknowledge the Universiti Kebangsaan Malaysia (UKM) and the Malaysian Government for their sponsorship under Grant (nos. UKM-AP-NBT-14–2010 and OUP-2012-075). The first author also acknowledges Japan–Malaysia Technical Institute and the Public Service Department of Malaysia for their support on the author's graduate studies.

References

[1] R.M. German, Powder Injection Molding, Metal Powder Industries Federation, Princeton, NJ, 1990.

[2] Z.Y. Liu, N.H. Loh, S.B. Tor, K.A. Khor, Y. Murakoshi, R. Maeda, Binder system for micropowder injection molding, Materials Letters 48 (2001) 31–38.

[3] Iriany, Rheological Study of Metal Injection Molding Feedstock Containing Palm Stearine, Ph.D. thesis, Universiti Kebangsaan Malaysia, 2002.

[4] K.F. Hens, D. Kupp, Advanced production methods for PIM feedstocks, Proceedings of the Advances in Powder Metallurgy and Particulate Materials 6 (1995) 45–54.

[5] Y. Li, L. Li, K.A. Khalil, Effect of powder loading on metal injection molding, Journal of Materials Processing Technology 183 (2007) 432–439.

[6] J.Y. Roh, J. Kwon, C.S. Lee, J.S. Choi, Novel fabrication of pressure-less sintering of translucent powder injection molded (PIM) alumina blocks, Ceramics International 37 (2011) 321–326.

[7] P. Thomas-Vielma, A. Cervera, B. Levenfeld, A. Varez, Production of alumina parts by powder injection molding with a binder system based on high density polyethylene, Journal of the European Ceramic Society 28 (2008) 763–771.

[8] J. Cheng, W. Lei, C. Yanbo, Z. Jinchuan, S. Peng, D. Jie, Fabrication of W–20 wt%Cu alloys by powder injection molding, Journal of Materials Processing Technology 210 (2010) 137–142.

[9] M. Trunec, J. Cihlar, Thermal removal of multicomponent binder from ceramic injection mouldings, Journal of the European Ceramic Society 22 (2002) 2231–2241.

[10] S.M. Ani, A. Muchtar, N. Muhamad, J.A. Ghani, Optimum powder loading of feedstock based on an alumina–zirconia powder for ceramic injection molding, Advanced Materials Research 686 (2013) 275–279.

[11] R.M. German, A. Bose, Injection Molding for Metals and Ceramics, Metal Powder Industries Federation, Princeton, NJ, 1997.

[12] B.C. Mutsuddy, R.G. Ford, Ceramic Injection Molding, Chapman and Hall, London, 1995.

[13] R. Supati, N.H. Loh, K.A. Khor, S.B. Tor, Mixing and characterization of feedstock for powder injection molding, Materials Letters 46 (2000) 109–114.

[14] D.M. Liu, W.J. Tseng, Rheology of injection-molded zirconia–wax mixtures, Journal of Materials Science 35 (2000) 1009–1016.

[15] M.E. Sotomayor, A. Varez, B. Levenfeld, Influence of powder particle size distribution on rheological properties of 316 L powder injection moulding feedstocks, Powder Technology 200 (2010) 30–36.

[16] R.M. German, Prediction of sintered density for bimodal powder mixtures, Metallurgical Transactions 23A (1992) 1455–1465.

[17] N. Murtadhahadi, C.H. Muhamad, Che Harun, Influence of injection parameters for SS316L, PEG, PMMA and stearic acid material, Journal of Applied Technology 3 (2005) 26–35.

[18] S.M. Ani, A. Muchtar, N. Muhamad, J.A. Ghani, Effects of injection temperature and pressure on green part density for ceramic injection molding, Advances in Materials Research 622–623 (2013) 429–432.

[19] T. Zhang, J.R.G. Evans, The solidication of large sections in ceramic injection molding: Part I conventional molding, Journal of Materials Research 8 (1993) 187–194.

[20] Murtadhahadi, Injection Parameter for Metal Injection Molding (MIM) Process to Make Use of Feedstock of SS 316 L, PEG, PMMA and Stearic Acid, M.Sc. thesis, Universiti Kebangsaan Malaysia, 2007.

[21] F. Mohd Foudzi, N. Muhamad, A.B. Sulong, H. Zakaria, Yttria stabilized zirconia formed by microceramic injection molding: rheological properties and debinding effects on the sintered part, Ceramics International 39 (2013) 2665–2674.

[22] I. Cristofolini, A. Rao, C. Menapace, A. Molinari, Influence of sintering temperature on the shrinkage and geometrical characteristics of steel parts produced by powder metallurgy, Journal of Materials Processing Technology 210 (2010) 1716–1725.

[23] R.V. Mangalaraja, B.K. Chandrasekhar, P. Manohar, Effect of ceria on the physical, mechanical and thermal properties of yttria stabilized zirconia toughened alumina, Materials Science and Engineering: A 343 (2003) 71–75.

[24] M. Ipek, S. Zeytin, C. Bindal, An evaluation of $Al2O_3$–ZrO_2 composites produced by coprecipitation method, Journal of Alloys and Compounds 509 (2011) 486–489.